

Supplementary files

TET1s deficiency exacerbates oscillatory shear flow-induced atherosclerosis

Kai Qu¹, Caihong Wang¹, Lu Huang¹, Xian Qin¹, Kun Zhang¹, Yuan Zhong¹, Qingfeng Ma¹, Wenhua Yan¹,
Tianhan Li¹, Qin Peng², Yi Wang¹, Hans Gregersen^{1,3}, Chaojun Tang⁴, Juhui Qiu^{1,*}, Guixue Wang^{1,*}

1. Key Laboratory for Biorheological Science and Technology of Ministry of Education, State and Local Joint Engineering Laboratory for Vascular Implants, College of Bioengineering Chongqing University, Chongqing, China;
2. Institute of Systems and Physical Biology, Shenzhen Bay Laboratory, Shenzhen, China;
3. GIOME, Department of Surgery, the Chinese University of Hong Kong, Hong Kong, China.
4. Cyrus Tang Hematology Center, Collaborative Innovation Center of Hematology, Soochow University, Suzhou, China.

*Corresponding author. Email: wanggx@cqu.edu.cn (Gui-xue Wang); jhqu@cqu.edu.cn (Ju-hui Qiu)

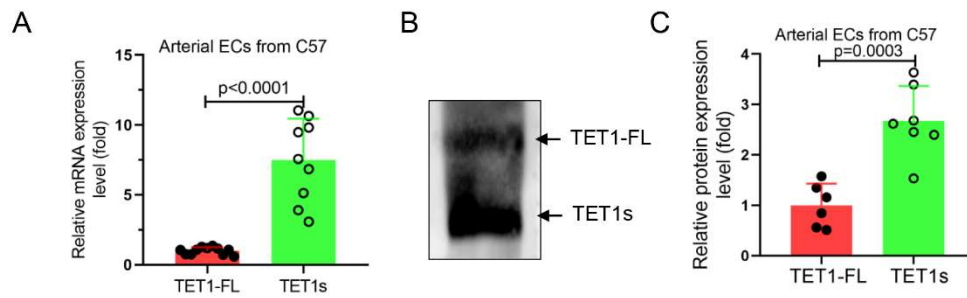


Figure S1. TET1s is the predominant transcript compared to TET1-FL in arterial ECs from C57 mice. (A-C) All ECs separated from the aorta of C57 mice. (A) RT-qPCR was used to test the mRNA levels of TET1s and TET1-FL ($n > 6$ per group). (B-C) The TET1s and TET1-FL protein expression level was quantified by WB ($n > 6$ per group). All data were presented as the mean \pm SD.

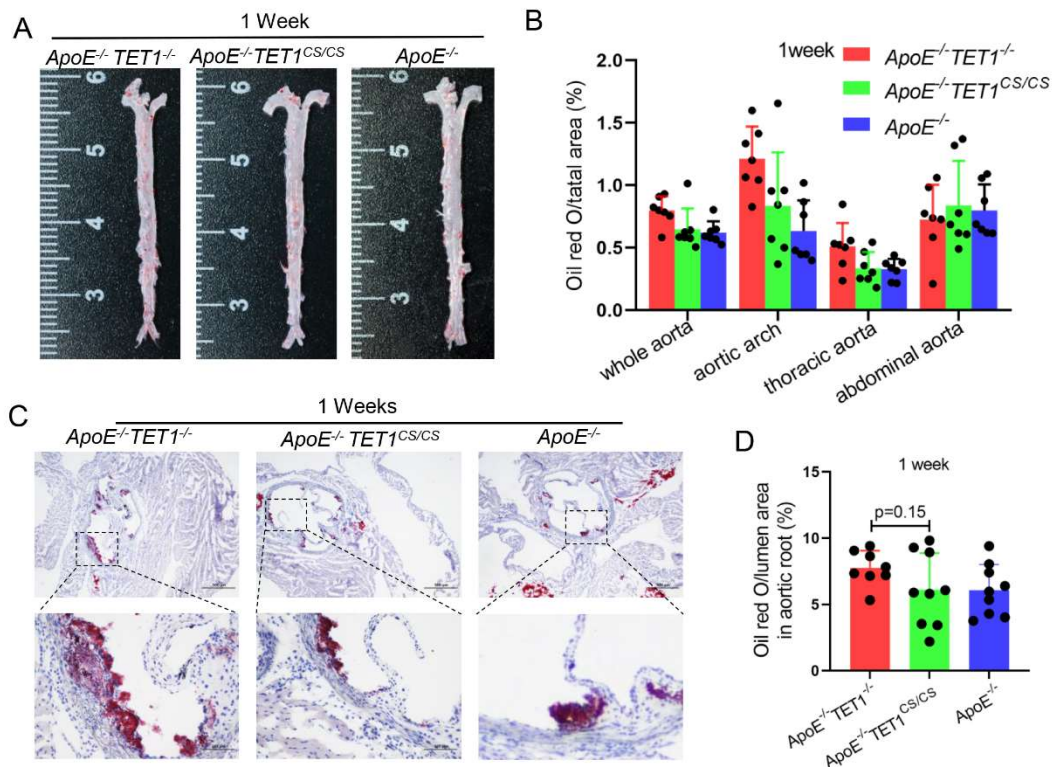


Figure S2. The plaques in *ApoE*^{-/-}*TET1*^{cs/cs} mice was no difference compared with *ApoE*^{-/-}*TET1*^{-/-} mice fed a high-fat diet for 1 week. (A-D) *ApoE*^{-/-} *TET1*^{-/-}, *ApoE*^{-/-} *TET1*^{cs/cs} and *ApoE*^{-/-} mice (8 weeks old) were fed a high-fat diet for 1 weeks. (A) The aortic plaques of *ApoE*^{-/-} *TET1*^{-/-}, *ApoE*^{-/-} *TET1*^{cs/cs} and *ApoE*^{-/-} mice were tested by red oil staining and en face microscopy. (B) The lesion areas in the whole aorta, aortic arch, thoracic aorta, and abdominal aorta sections were

analyzed ($n > 7$ per group). (C-D) Representative photomicrographs of aortic root slice red oil staining and quantitative analysis of atherosclerotic plaque areas in the aortic root ($n > 7$ per group). All data were presented as the mean \pm SD.

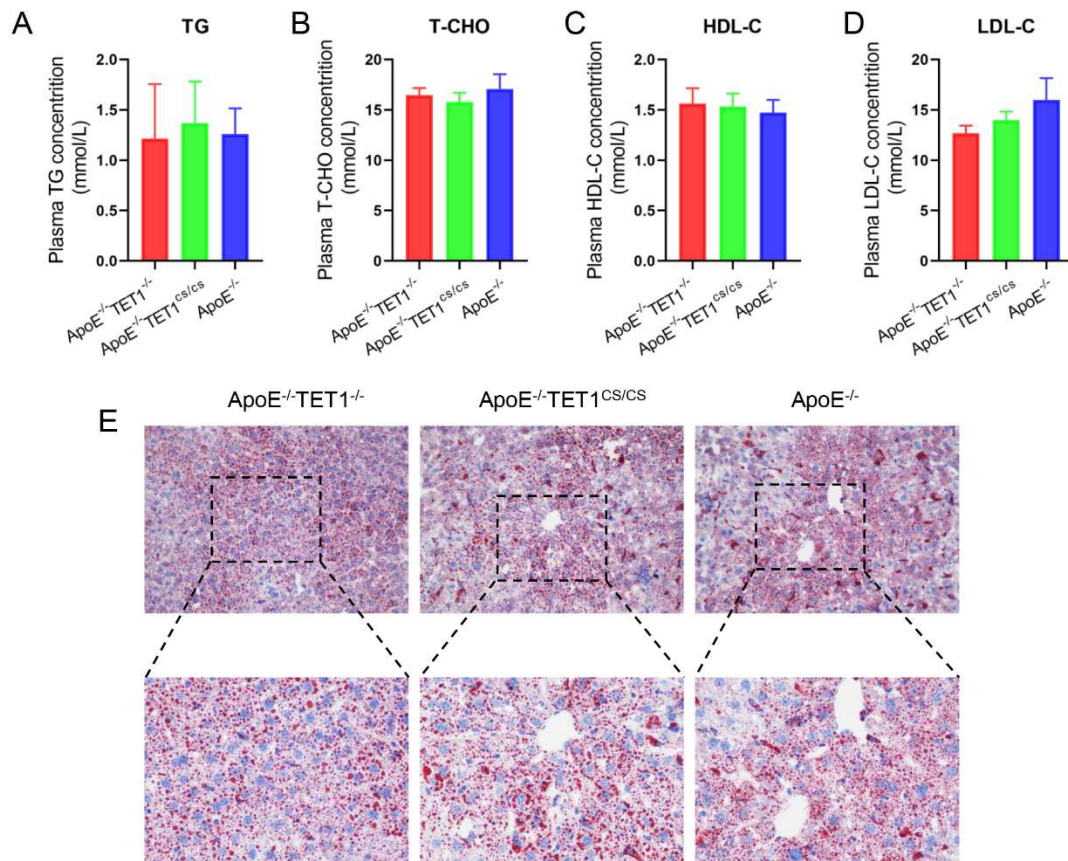


Figure S3. Deletion of TET1s has no significant change in lipid metabolism in ApoE^{-/-} mice. (A-E) ApoE^{-/-}TET1^{-/-}, ApoE^{-/-}TET1^{CS/CS} and ApoE^{-/-} mice fed with high-fat diet for 12 weeks. (A) Quantitative analyze in triglyceride (TG) of ApoE^{-/-}TET1^{-/-}, ApoE^{-/-}TET1^{CS/CS} and ApoE^{-/-} mice fed with high-fat diet for 12 weeks. (A-D) Quantitative analyze triglyceride (TG), total cholesterol (T-CHO), LDL-C and HDL-C of ApoE^{-/-}TET1^{-/-}, ApoE^{-/-}TET1^{CS/CS} and ApoE^{-/-} mice (E) The representative images with hepatic slice staining with oil red O of ApoE^{-/-}TET1^{-/-}, ApoE^{-/-}TET1^{CS/CS} and ApoE^{-/-} mice. All data are presented with mean value and standard deviation (SD).

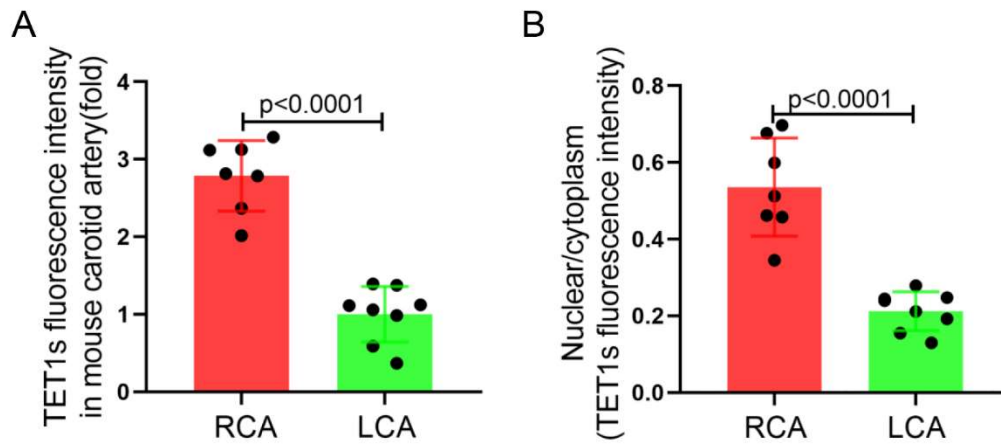


Figure S4. OSS stimulation was decreased the expression and the nuclear/cytoplasmic ratio of TET1s in carotid ECs in TET1^{es/cs} mice. (A-B) TET1^{es/cs} mice LCA were ligated for 2 weeks. (A) Quantitative analysis of TET1s fluorescence intensity in LCA and RCA ECs to fig.3B. (B) Quantitative analysis of the nuclear/cytoplasmic ratio of TET1s in LCA and RCA ECs to fig.2B. All data were presented as the mean \pm SD.

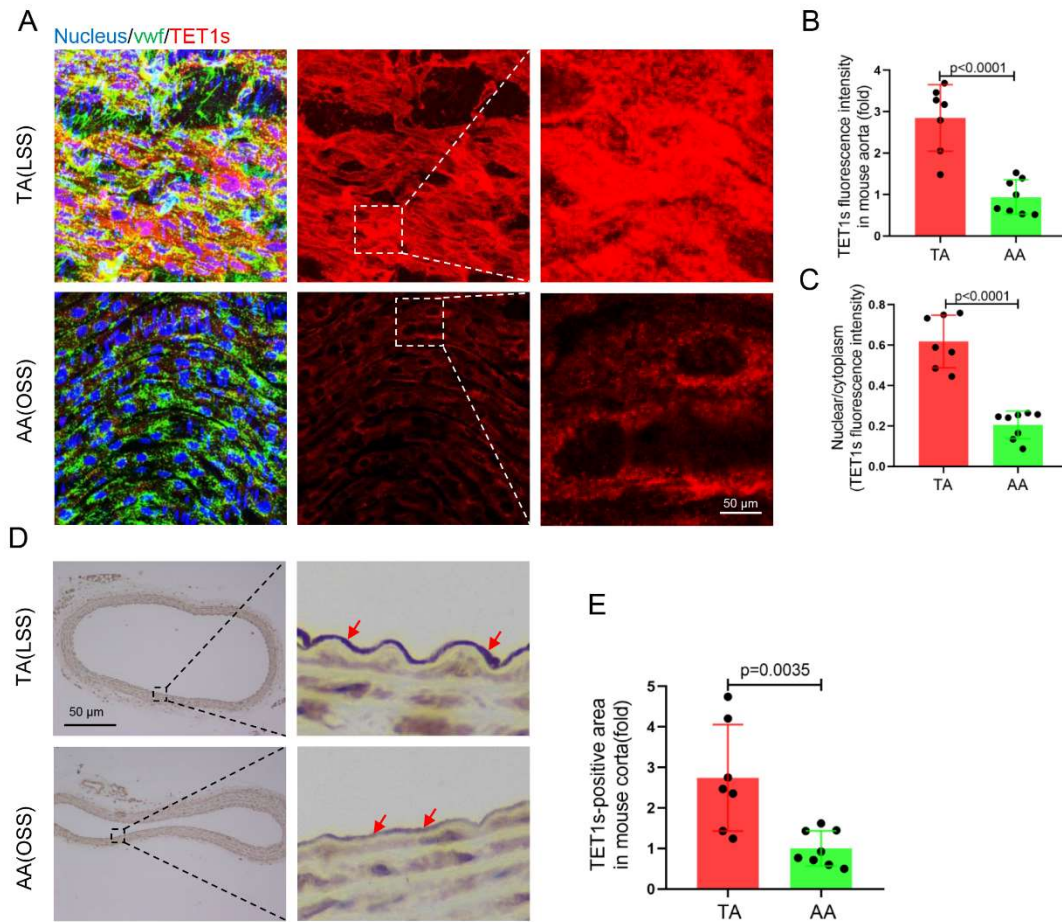


Figure S5. OSS stimulation was decreased the expression and the nuclear/cytoplasmic ratio of TET1s in aortic ECs in TET1^{cs/cs} mice. (A) Immunofluorescence staining & *en face* for TET1s in AA and TA ECs (n>7 per group). (B-C) Quantitative analysis of the fluorescence intensity and the nuclear/cytoplasmic ratio of TET1s in AA and TA ECs (n>7 per group). (D-E) Immunohistochemical staining for TET1s in AA and TA slices and quantitative analysis of the TET1s-positive area; red arrows indicate the positive area in ECs (n>7 per group). All data were presented as the mean \pm SD.

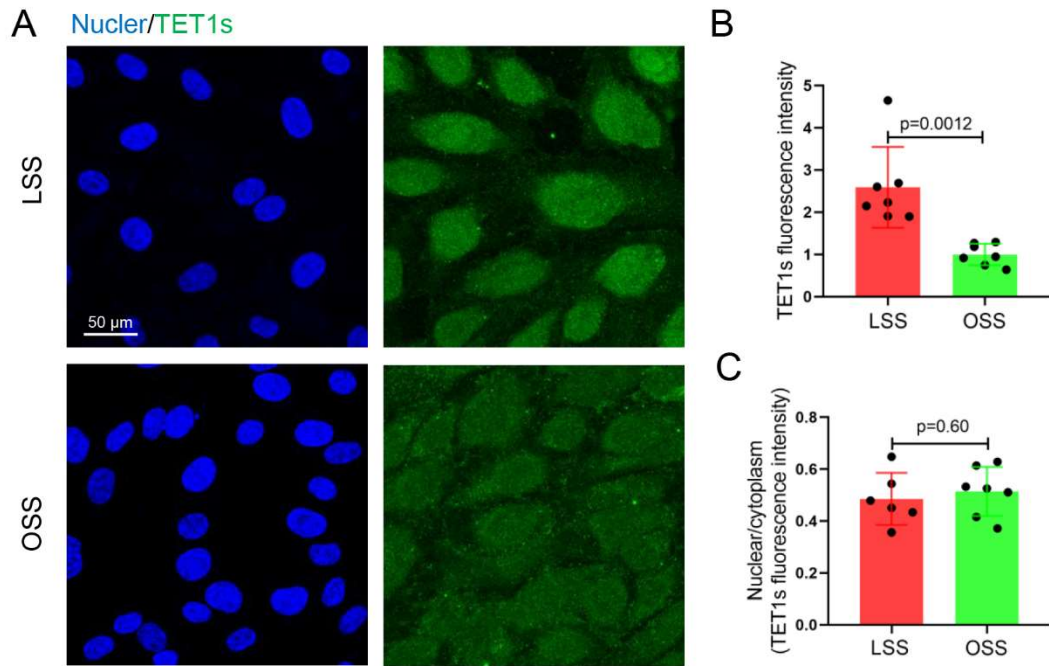


Figure S6. OSS inhibits TET1s expression levels in primary HUVECs. (A-C) primary HUVECs with a parallel-plate flow chamber (PPFC) for 24 h. (A) Immunofluorescence staining for TET1s in p-HUVECs. (B-C) Quantitative analysis of the fluorescence intensity and the nuclear/cytoplasmic ratio of TET1s in p-HUVECs (n=7 per group). All data were presented as the mean \pm SD.

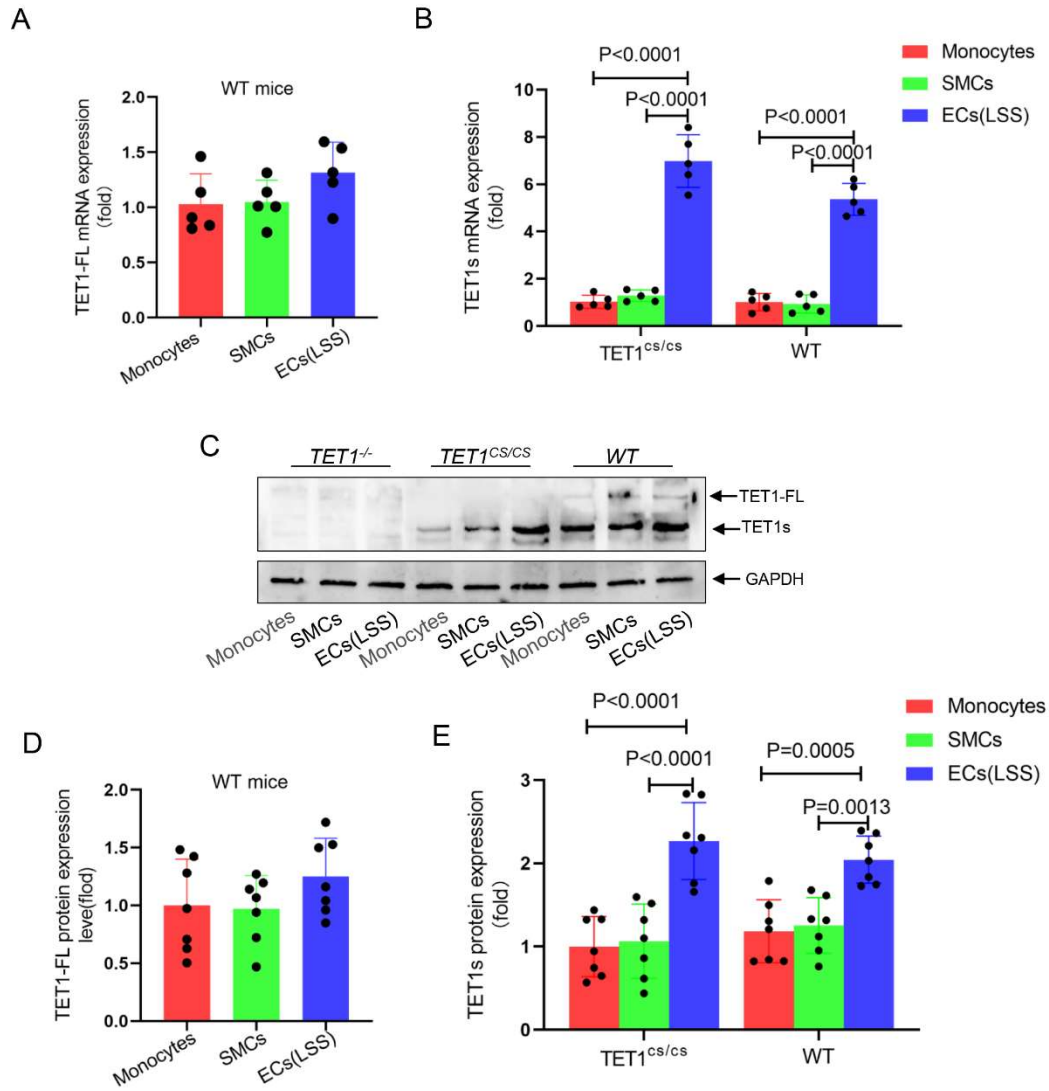


Figure S7. Low expression levels of TET1s in vascular smooth muscle cells and macrophages.

(A-C) All ECs separated from the thoracic aorta (TA) of TET1^{-/-}, TET1^{cs/cs} and WT mice. (A-B) RT-qPCR was used to test the mRNA levels of TET1s and TET1-FL (n=4 per group). (C) The TET1s and TET1-FL protein expression level was quantified by WB (n=4 per group). All data were presented as the mean ± SD.

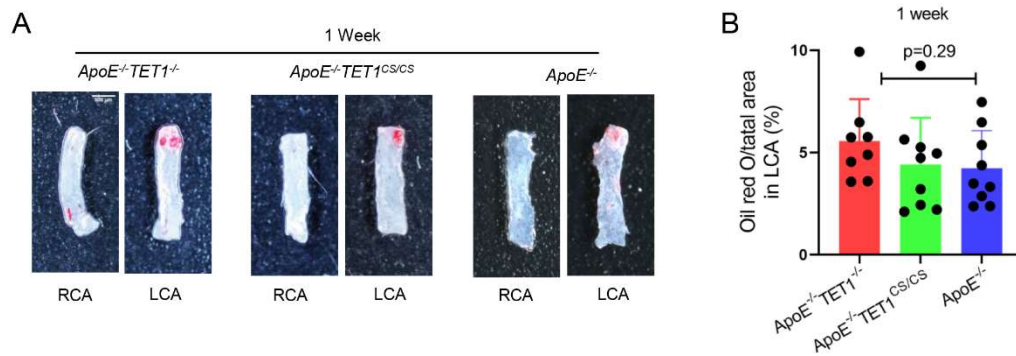
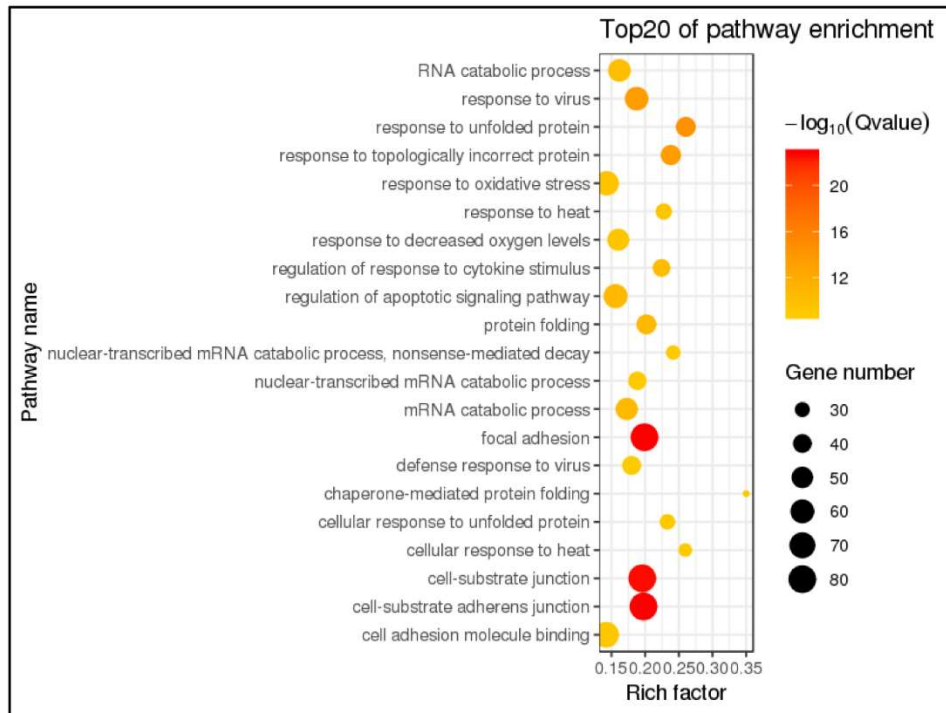


Figure S8. The carotid plaques in *ApoE^{-/-}TET1^{cs/cs}* mice with a partial carotid artery ligation is no difference compared with *ApoE^{-/-}TET1^{-/-}* mice fed a high-fat diet for 1 week. (A-B) *ApoE^{-/-}TET1^{cs/cs}*, *ApoE^{-/-}TET1^{-/-}* and *ApoE^{-/-}* mice LCAs were ligated and fed a high-fat diet for 1 week; the lesion areas in the carotid artery were tested by red oil stain & en face and were analyzed (n=8 per group). All data were presented as the mean \pm SD.

A



B

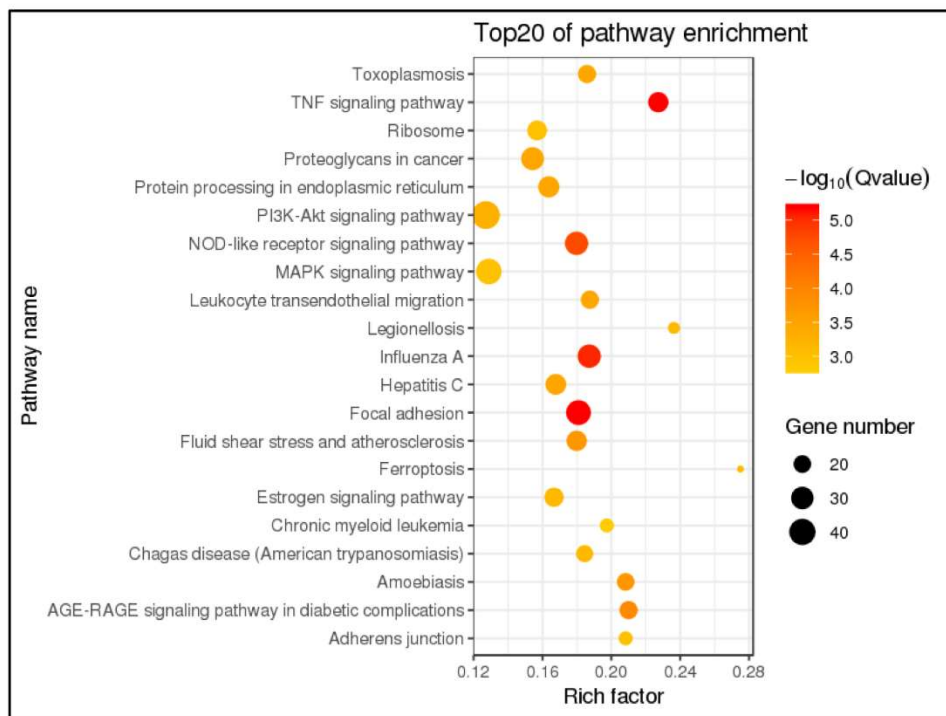


Figure S9. Differential gene expression enrichment analysis shows that TET1s may regulate endothelial barrier function. (A-B) RNA sequencing test the global RNA levels of TET1s-overexpressing p-HUVECs and negative control p-HUVECs; the top 20 pathways of differential gene expression GO enrichment analysis (A) and KEGG enrichment analysis (B) with RNA-

sequence data.

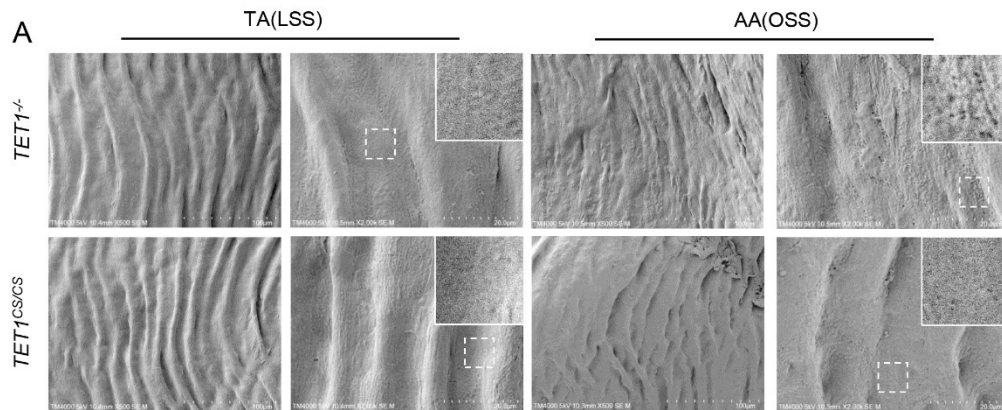


Figure S10. The intima of the aortic arch of $TET1^{cs/cs}$ mice shows fewer holes compared with $TET1^{-/-}$ mice. (A) The morphology of ECs in AA and TA ECs by scanning electron microscopy (SEM).

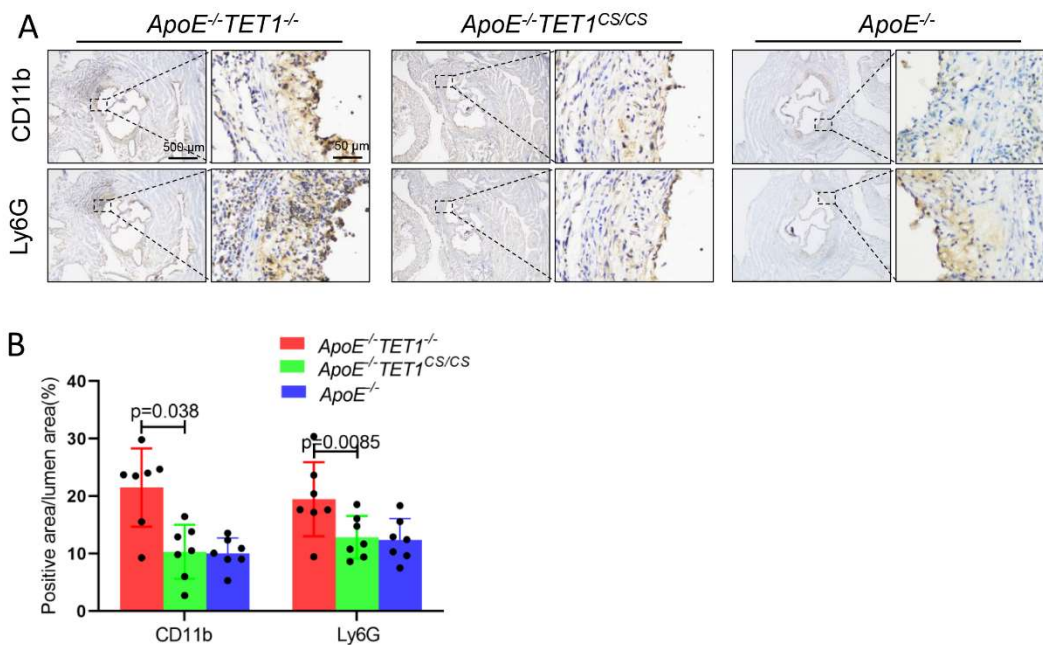


Figure S11. Neutrophils were significantly decreased in the plaques of $ApoE^{-/-}TET1^{cs/cs}$ mice compared with $ApoE^{-/-}TET1^{-/-}$ mice. (A-B) $ApoE^{-/-}TET1^{cs/cs}$, $ApoE^{-/-}TET1^{-/-}$ and $ApoE^{-/-}$ mice were fed a high-fat diet for 4 weeks. The aortic roots were harvested and subjected to further experiments. Representative immunohistochemical staining for Neutrophil-specific antigens CD11b and Ly6G in aortic roots and were analyzed (n=6 per group). All data are presented as the

mean \pm SD.

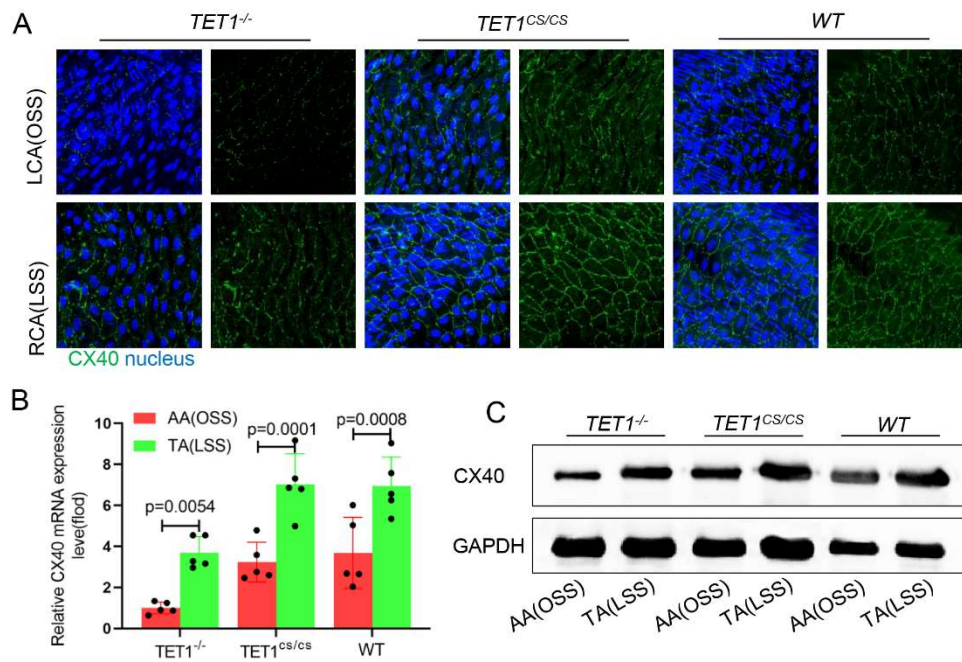


Figure S12. The endothelial CX40 expression level in *TET1*^{-/-} and *TET1*^{cs/cs} mice. (A) *TET1*^{-/-}, *TET1*^{cs/cs} and *WT* mice LCAs were ligated for 1 week. Immunofluorescence staining for CX40 in RCA and LCA (n=3 per group). (B-C) All ECs separated from the aortic arch (AA) and thoracic aorta (TA) of *TET1*^{-/-}, *TET1*^{cs/cs} and *WT* mice. (B) RT-qPCR was used to test the mRNA levels of CX40 (n=5 per group). (C-D) The CX40 protein expression level was quantified by WB (n=4 per group). All data were presented as the mean \pm SD.

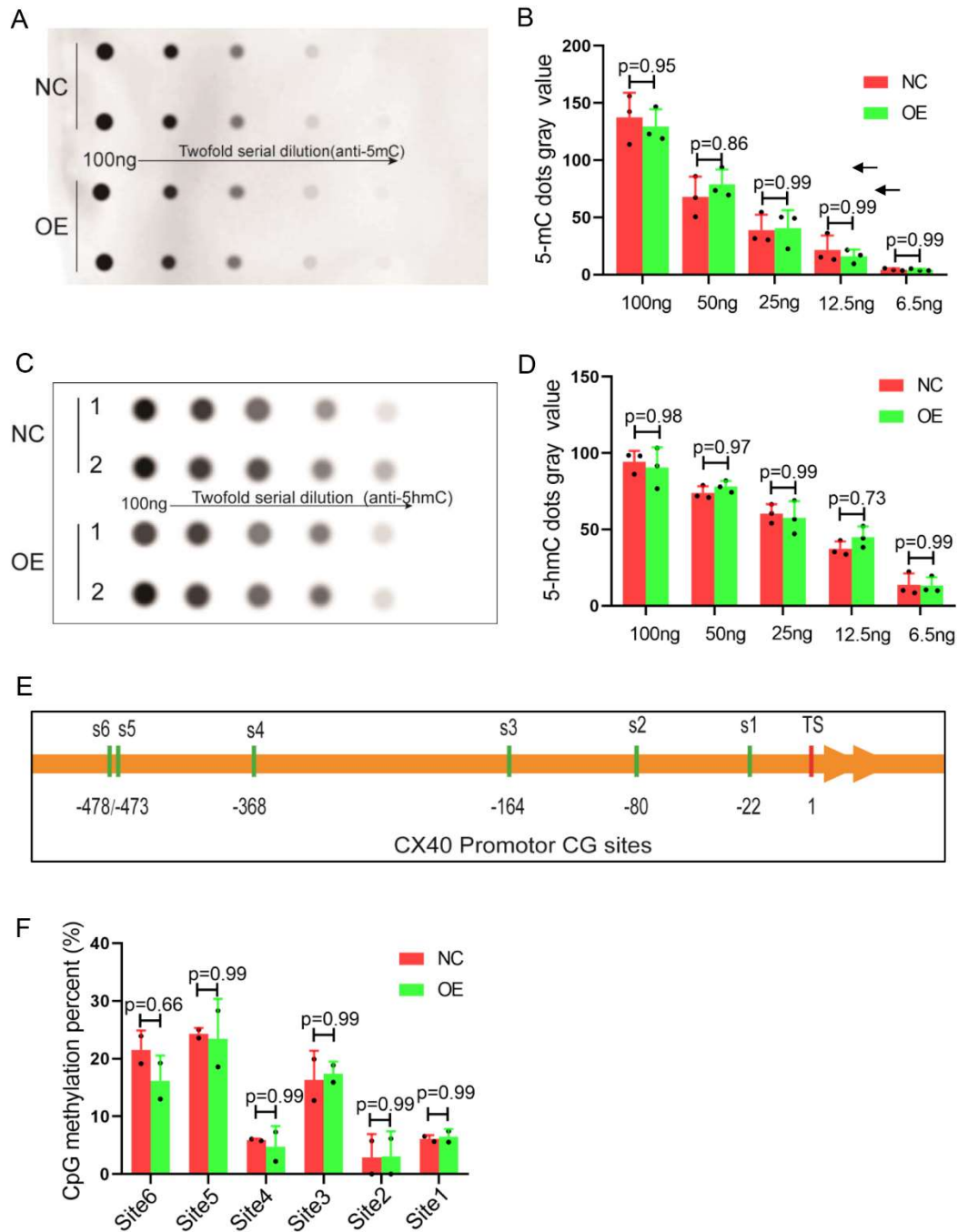


Figure S13. TET1s overexpression did not cause a global difference in 5mC levels in p-HUVECs. (A-F) p-HUVECs were transfected with TET1s-overexpressing adenovirus and negative control adenovirus and further tested after 48 h. (A-B) Dot blot assay was used to analyze the global 5mC levels of p-HUVECs (n=6 per group). (C-D) Dot blot assay was used to analyze the global 5hmC levels of p-HUVECs (n=6 per group). (E-F) Pyrosequencing assay analyzed the local 5hmC levels in the CX40 promoter 6 CG sites (S1-S6 indicates site 1-site 6; TS indicates transcriptional start; n=3 per group). All data were presented as the mean \pm SD.

Table S1. The primers for gene-test of knockout mice.

primers (name)	sequence(5'-3')
GT-apoE-OF	GCCTAGCCGAGGGAGAGCCG
GT-apoE-IR	TGTGACTTGGGAGCTCTGCAGC
GT-apoE-OR	GCCGCCCGACTGCATCT
GT-TET1-F	AACTGATTCCCTTCGTGCAG
GT-TET1-R	TTAAAGCATGGGTGGGAGTC
GT-TET1CS-OF	ATCTGGGCAATGTTGTGACTC
GT-TET1CS-IR	CATTGTAAACCCGTTGCAAGT
GT-TET1CS-OR	TTCTTCCCTTCCACTATGCA

Table S2. The primers for RT-qPCR.

primers (name)	sequence(5'-3')
H-GAPDH-F	GGAGCGAGATCCCTCCAAAAT
H-GAPDH-R	GGCTGTTGTCATACTTCTCATGG
H-TET1FL-F	GCGCGAGTTGGAAAGTTTG
H-TET1FL-R	GCTCAGTCACACAAGGTTTTGG
H-TET1s-F	CAAGCAAGATGGCTACCTCGT
H-TET1s-R	GGGGCCTCTTGTTTTCCCTTA
H-CX40-F	GCTGCCAGAATGTCTGCTAC
H-CX40-R	GGTACTCGTAAGAGCCAGAGC
H-TMEM129-F	GAGGTGACCTTCACTCTCGC
H-TMEM129-R	GCCCACATAGTAGCCGAGC
H-TGFA-F	AGGTCCGAAAACACTGTGAGT
H-TGFA-R	AGCAAGCGTTCTTCCCTTC
H-IGF1-F	GCTCTTCAGTTCGTGTGTGGA

H-IGF1-R	GCCTCCTTAGATCACAGCTCC
H-APLNR-F	CCTGCATCAGCTACGTCAACA
H-APLNR-R	GGGATGGATTTCTCGTGCATCT
H-PIEZO2-F	ATGGCCTCAGAAGTGGTGTG
H-PIEZO2-F	ATGCCTTGCATCGTCGTTTT
H-KLF2-F	CTACACCAAGAGTTCGCATCTG
H-KLF2-R	CCGTGTGCTTTCGGTAGTG
H-KLF4-F	CAGCTTCACCTATCCGATCCG
H-KLF4-R	GACTCCCTGCCATAGAGGAGG
M-TET1FL-R	TACTGCAAGAATCGAAAGAACAGCCA
M-TET1FL-R	CGGAAGGTGTGTGTCAGTGGGT
M-TET1s-F	TAAGACAGACTTTTAGGGGGAAAG
M-TET1s-R	GTGTGTGTCAGTGGGTAAACAGT
M-GAPDH-F	TGACCTCAACTACATGGTCTACA
M-GAPDH-R	CTCCCATCTCGGCCTTG
M-CX40-F	GGTCCACAAGCACTCCACAG
M-CX40-R	CTGAATGGTATCGCACCGGAA

Table S3. The primers for CHIP- qPCR.

primers (name)	sequence(5'-3')
P1-F	TCCTGTCACTGAGGAAATTCCTGTTC
P1-R	TGCTGTCTGAGATGGCTCTTAATGAG
P2-F	TCATTAAGAGCCATCTCAGACAGCAG
P2-R	AATCTCTGATGCTGGCCTTGC
P3-F	AAGGCAAGGCCAGCATCAG
P3-R	TCCTGTGCATGACTTTCTGGAATG
P4-F	CTCATTCCAGAAAGTCATGCACAGG
P4-R	GCCTGAAGTCAAGCTTGTCTGG
P5-F	CCAGACAAGCTTGACTTCAGGC

P5-R	GAGATCTTGCCTGAGAGCATTATGCTC
------	-----------------------------

Table S4. The primers for pyrosequencing assays.

primers (name)	sequence(5'-3')
1.GJA5-1F(230bp)	TTTGGGTGAAAGTTTATTGGATATG
1.GJA5-1R	TCCCAACTTTAATCTACTCCTATCACT
1.GJA5-1S	CTCAAAAACATTTAACTTCC
2.GJA5-2F(72bp)	TGGTTTTTGGGTGAAAGTTT
2.GJA5-2R	AAACCATCTCAAACAACAAATATCTATTAA
2.GJA5-2S	TTTTGGGTGAAAGTTTATT
3.GJA5-3F(224bp)	AGAGGATTAGAAAAGGTAAGGTTAGTAT
3.GJA5-3R	CCTCTTTAAAACCTAAAATCAAACCTATCT
3.GJA5-3S	AGAGGTTTTTAAGTAAATAGTG
4.GJA5-2F(221bp)	AAGGAGATTTTGTTTTGAGAGTATTATG
4.GJA5-4R	AACAATACTACCCATCCTTTCAACTACCC
4.GJA5-4S	ATTAAAAAGGAAGTTAGATTGT
5.GJA5-5F(140bp)	TGATTTTAGGTTTAAAGAGGAAGTTAATG
5.GJA5-5R	ACTCAACCCTTCCCTAAC
5.GJA5-5S	ACCCTTCCCTAACTC